scientific reports

OPEN

Insight into the dynamics of second grade hybrid radiative nanofluid flow within the boundary layer subject to Lorentz force

Muhammad Jawad[1], Anwar Saeed[1], Asifa Tassaddiq[2], Arshad Khan[3], Taza Gul[4], Poom Kumam[5,6]✉ & Zahir Shah[7]✉

The magnetohydrodynamic hybrid second-grade nanofluid flow towards a stretching/shrinking sheet with thermal radiation is inspected in current work. Main concern of current investigation is to consider hybrid $Al_2O_3 - Cu$ nanofluid which is perceived by hanging two dissimilar kinds of nanoparticles known as alumina and copper within the base fluid. The fluid motion is produced by non-linear stretching/shrinking sheet. The modeled equations which comprise of energy, motion and continuity equations are changed into dimensionless form using group of similar variables. To determine the solution of transformed problem, the Homotopy Analysis technique is used. The findings of this work revealed that the magnetic parameter improves the heat transfer rate. This work also ensures that there are non-unique solutions of modeled problem for shrinking case and a unique solution for stretching case. Higher values of Re_x results in declining of flow field. Rise in M agrees to a decline in velocity distributions. Higher values of second order fluid parameter reduces the viscosity of fluid and accordingly velocity increases. Velocity profile is also a decreasing function of volume friction.

Abbreviations

u, v	Velocity components
x, y	Cartesian coordinates
T	Hybrid nanofluid temperature
λ	Constant parameter
T_∞	Ambient temperature
M	Magnetic parameter
T_w	Wall temperature
β_1	Dimensionless parameter
θ_w	Temperature ratio parameter
ρ_{hnf}	Density of hybridnanofluid
ν_{hnf}	Kinematic viscosity of hybridnanofluid
α_{hnf}	Thermal diffusivity of hybridnanofluid
$(\rho c_p)_{hnf}$	Heat capacity of hybridnanofluid
S_1, S_2	Transpiration parameters
Ec	Eckert number

[1]Department of Mathematics, Abdul Wali Khan University, Mardan 23200, Khyber, Pakhtunkhwa, Pakistan. [2]Department of Basic Sciences and Humanities, College of Computer and Information Sciences, Majmaah University, Al-Majmaah 11952, Saudi Arabia. [3]College of Aeronautical Engineering, National University of Sciences and Technology (NUST), Sector H-12, Islamabad 44000, Pakistan. [4]Department of Mathematics, City University of Science and Information Technology, Peshawar 25000, Khyber, Pakhtunkhwa, Pakistan. [5]Fixed Point Research Laboratory, Fixed Point Theory and Applications Research Group, Center of Excellence in Theoretical and Computational Science (TaCS-CoE), Faculty of Science, King Mongkut's University of Technology Thonburi (KMUTT), 126 Pracha Uthit Rd., Bang Mod, Thung Khru, Bangkok 10140, Thailand. [6]Center of Excellence in Theoretical and Computational Science (TaCS-CoE), Faculty of Science, King Mongkut's University of Technology Thonburi (KMUTT), 126 Pracha Uthit Rd., Bang Mod, Thung Khru, Bangkok 10140, Thailand. [7]Department of Mathematical Sciences, University of Lakki Marwat, Lakki Marwat 28420, Khyber Pakhtunkhwa, Pakistan. ✉email: poom.kum@kmutt.ac.th; zahir@ulm.edu.pk

R	Radiation parameter
C_{fx}	Skin friction coefficient
τ_w	Shear stress
B_0	Strength of magnetic field
β	Second grade fluid parameter
Nu_x	Nusselt number
Re_x	Reynolds number
Pr	Prandtl number
L	Characteristic length of the sheet
f'	Dimensionless velocity
∞	Ambient condition
w	Condition on surface
$'$	Derivative with respect to η

Nanofluid receives an enormous amount of attention over the last two decades by the researchers because of its high thermal conductivity and novel applications in different branches of science, engineering and technology. The conventional liquids consume low thermal conductivity thus it becomes inadequate for several heat transfer issues. The study of nanofluid is very important for the reason of its unique application that enhances the transfer of heat. That's why scientists take interest to use nanofluid instead of regular fluids. Nanofluid shows a vital role at manufacturing level such as production of foods, electronics, biomedicines, transportations and cooling of nuclear reactors. Nanoparticles are very small in size (1–100 nm). The structure of nanoparticles contains a metal oxide, nitride, carbide and carbon tubes (SWCNTs and MWCNTs) etc. The quantity of nanopraticles in a base fluid was introduced first by Choi[1] for increasing the thermal characteristics of such fluids. These fluids with heightened thermophysical properties were named as nanofluids. There are different types of nanofluids like fermium oxide, grapheneoxide, and carbon nanotubes etc. which are discussed in the literature. In the setting of medical flows, Akbar et al.[2] utilized Buonjiornio's model to explore systematically the peristaltic hydrodynamics of nanoliquids with wall slip impacts. Sayed et al.[3] studied the influence of thermal transportation and alternative current on the peristaltic flow of a viscous dielectric fluid. Nakhchi and Esfahani[4] examined a mathematical investigation for Cu–water nanoliquid flow through a spherical cylinder implanted with cross-cut warped tape with an alternative axis (CCTA). Furthermore, the reader can study about nanofluid in Refs.[5–7].

Carbon nanotubes (CNTs) are round and hollow formed cylinders with indispensable qualities like great thermal conductivity and huge power makes them exceptionally appealing constituents in fluctuated applications for instance enhancer, drug delivery, optics and semiconductors etc. CNTs can be single or multi wall. Homogeneous carbon nanotube/polymer composites utilizing non-covalently functionalized, solvent single-walled carbon nanotubes (SWNTs) were created by Ramasubramaniam et al.[8]. Xue[9] offered the carbon nanotubes (CNTs) alignment dissemination a new model of active thermal conductivity of CNTs. The study of SWCNT on peristaltic transportation of nanofluid in an inclined cylinder with penetrable walls is conferred by Nadeem et al.[10]. Homogeneous-heterogeneous reactions in the 3D flow of water-based nanoliquid soaking a permeable medium are demonstrated by Hayat et al.[11]. Nadeem et al.[12] observed the transfer of heat by the influence of SWNCT and MWNCT with the state of oscillation. Late examinations featuring nanofluid impacts in different situations might be found in Ref.[13,14]. Various mathematical models have been used by the researcher over the linear stretched surfaces while limited work has been carried out in nonlinear or quadratic stretching.

The fluid of second grade is actually a subclass of non-Newtonian fluid for which flow field has a relationship up to second order derivative in terms of stress strain tensor. On the other hand, this relationship is of first order in case of the Newtonian fluids. Due to its importance, many researchers have diverted their attention towards the flow of second grade fluid. The study of thermal flow regarding this type of fluid is of more importance for researchers these days. The second grade liquid flow past a quadratic stretched surface analyzed by Cortell[15,16]. This idea further comprehended by Mahapatra and Sidui[17]. Gul et al.[18] considered steady, axisymmetric and incompressible hybrid Nano liquid flow over an unending impermeable gyrating disk affected by a magnetic field, which has a few engineering and industrial applications. Sheikholeslami et al.[19] discovered unsteady squeezing liquid flow amid corresponding surfaces. They reported that heat transfer escalates for nanoparticle concentration. Jawad et al.[20] have deliberated the impression of variable thermal radiation over the unsteady 3-D flow of (SWCNTs) with water-base solutions.

A unique type of nanofluid that formed small metallic particles is called hybrid nanofluid. Hybrid nanofluid shares great applications in the field of engineering, agriculture, biological and applied sciences. Hybrid nanofluid increases the thermal efficiency at a very low cost. The electromagnetic radiation caused by the thermal flow of particles in the matter is termed as thermal radiation. These types of radiations are emitted by those matters which have a temperature higher than absolute zero. The motion of particles results in a charge acceleration that causes electromagnetic radiations. The use of hybrid nanofluid is more fruitful because their applications involve diesel engine oil, hybrid power engines, chillers improvement etc. Due to the importance of this class of fluid many researchers have carried out numerous investigations in this area by using different flow conditions and geometries. The exploratory works by Turcu et al.[21] were the formerly contemplates that using the hybrid nanoparticles. Suresh et al.[22,23] led the exploratory effort utilizing $Al_2O_3 - Cu$ to examine the upgrade of the liquid thermal conductivity. Afterwards numerous investigators carried various studies for hybrid nanofluid by considering stretching/shrinking surfaces such as Waini et al.[24,25], Zainal et al.[26] and Khashi'ie et al.[27,28]. Relationships of thermal conductivity for ordinary nanofluids are completely examined and this study emphasizes planning, complications and challenges of hybrid nanofluids by Das[29]. Free convection of nanofluid in an inclined open cavity with a heat producing strong component is contemplated by Miroshnichenko et al.[30]. Siavashi and

Rostami[31] mathematically inspected the natural convection heat move of non-Newtonian water-nanoliquid inside a tube shaped annulus with a concentric round heat source secured with a conductive permeable layer. Huminic and Huminic[32] presented a research review of the current results used in different heat exchangers, concerning the thermophysical properties and the characteristics flow of the heat transfer in hybrid nanofluids. The review denotes that the hybrid nanofluids may significantly increase the performance of heat exchangers. However, lots of research efforts are still required considering the hybrid nanoparticles combinations, the exact mixing ratio and its stability. Dinarv[33] have presented torpor point limit layer flow of CuO–Ag/water hybrid nanoliquid. Dinarvand and Rostami[34] have calculated systematically the incompressible laminar steady 3-D limit layer flow of a watery hybrid nanoliquid over an impervious turning plate with the steady spiral extending rate. Tayebi and Chamkha[35] mathematically reviewed the heat transmission in an annulus between two confocal elliptic squares loaded up with hybrid $Al_2O_3 - Cu$/water nanoliquid. A completely evolved laminar convective heat transfer and weight drop attributes through a consistently heated round cylinder utilizing $Al_2O_3 - Cu$/water hybrid nanoliquid was introduced by Suresh et al.[36]. Jena et al.[37] explained the combination of nano-composites utilizing hydrogen reduction methods from synthetically articulated mixtures. Volume concentration and temperature on ethylene glycol and MWCNT with dynamics viscosity of hybrid nanofluids was achieved by Afshari et al.[38]. `Unsteady radiative ethylene glycol-based carbon nanotube flow between two revolving disks was inspected by Ramzan et al.[39]. They marked that radial velocity and temperature gets increased for nanoparticle concentration. Barnoon et al.[40] discussed rate of heat transmission with fluid flow using swirling circular obstacles. Afrand et al.[41] have investigated 3-D free convective flow through vertically cylindrical annulus using molten gallium. In this work the authors have used horizontal magnetic field. Barnoon et al.[42] have also discussed mixed convection with production of entropy using a square cavity where the cavity was filled with nanoparticles in the occurrence of magnetic effects. Farzinpour et al.[43] have discussed the simulation for molecular dynamics using effects of ferro-nanofluid and unsteady magnetic field effects. Mousavi et al.[44] have utilized the Lattice Boltzman method to explore the simulation of droplet detachment under the impact of electric field. Turkyilmazoglu et al.[45–48] have carried out a tremendous work for heat transfer using nanofluid with different flow geometries and various flow conditions. Shah et al.[49] have investigated the importance of suction and dual stretching on the motion of various types of nanofluids. Sheikholeslami et al.[50,51] have carried out a tremendous work for heat transmission of nanofluid. The reader can further study about heat transfer through nanofluid flow in Refs.[52–56].

The force exhibited by a particle due to magnetic and electric fields is termed as the Lorentz force. The force exerted on a particle due to the electric field is electric force and is given by the magnitude $F = qE$. On the other hand, a charged particle in a magnetic field will experience a force because of the magnetic field and is termed as a magnetic force where the particles are moving in a direction relative to the field motion. The combination of these two forces is termed as Lorentz force. Koriko et al.[57] have discussed the significance of using Fe_3O_4 nano-particles to alumina-water nanofluid past a stretching surface using Lorentz force. Vaidya et al.[58] have studied the MHD peristaltic flow for non-Newtonian fluid through a narrowing asymmetric channel. The transportation of fluid using variable transport properties carried out over a porous surface. Aly and Pop[59] have carried out the MHD flow of hybrid nanofluid flow past a shrinking/ stretching surface with a determination of double solution.

Most of the available literature is concern with the dispersion of the solid nanoparticles in the Newtonian fluids and very less literature available regarding the solid nano particles dispersion in the non-Newtonian fluids. In the current study we have focused the theoretical study of the non-Newtonian fluid considering the second grade fluid for the stable dispersion of the solid nanoparticles of $Al_2O_3 - Cu$.

The newness of the present work is highlighted in the following points.

- Second-grade fluid used as a base fluid.
- $Al_2O_3 - Cu$ are used as the solid nanoparticles.
- Magnetic field imposed vertically the flow pattern.
- Thermal radiation is included in the energy equation.
- The surface is nonlinearly stretching/shrinking.

Mathematical formulation

We assume here the steady MHD flow of an incompressible, electrically conducting Al2O3-Cu hybrid nanofluid towards a two-dimensional extending/shrinking sheet. Let x-direction is along the surface and y-axis being normal to the sheet along which magnetic field (B_0) is applied. The schematic diagram is depicted in Fig. 1.

The flow is likely to be formed by a quadratic (non-linearly) extending/contracting sheet, which are employed along x-axis and in this way sheet velocity is $u_w(x) = ax + bx^2$. By connecting with the assessments of the common limit layer, we can compose the hybrid nanofluid governing equations[15–17,55,56]:

$$u_x + v_y = 0, \tag{1}$$

$$uu_x + vu_y = \upsilon_{hnf}u_{yy} + \alpha_1\left(u_x u_{yy} + uu_{xyy} + u_y v_{yy} + vu_{yyy}\right) - \frac{\sigma_{hnf}B_0^2 u}{\rho_{hnf}}, \tag{2}$$

$$uT_x + vT_y = \frac{k_{hnf}}{(\rho c_p)_{hnf}}T_{yy} + \frac{16\sigma^*}{(\rho c_p)_{hnf}k^*}\left[T^3 T_{yy} + 3T^2(T_z)^2\right], \tag{3}$$

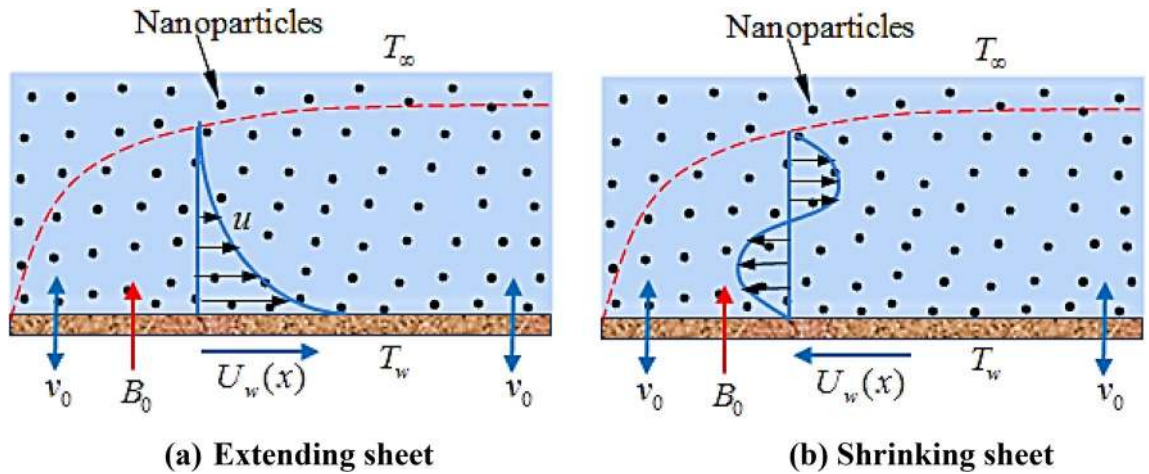Together with the boundary conditions[15–17,55,56]:

Figure 1. Physical sketch of the flow.

Physical properties	(Al_2O_3)	(Cu)
ρ (kg/m^3)	3970	8933
$B \times 10^{-5}$ (mK)	0.85	1.67
c_p (J/kgK)	765	385
k (W/mK)	40	400

Table 1. Numerical values of thermophysical properties of nanoparticles and pure fluid[26].

$$u = u_w(x) = \left(ax + bx^2\right)\lambda, \; v = v_w(x), T = T_w \, at \, y = 0,$$
$$u \rightarrow 0, T \rightarrow T_\infty, \qquad at \; y \rightarrow \infty. \tag{4}$$

Above u, v are the components of flow in x, y directions, λ is constant parameter with $\lambda > 0$ signifies that sheet is stretching while $\lambda < 0$ is a shrinking sheet. The value of T_w is depicted as $T_w(x) = T_\infty + T_\infty \left(\frac{x}{L^2}\right)$. The thermophoresis characteristics of alumina (Al_2O_3) and copper (Cu) are given in Table 1.

Thermophysical properties of hybrid nanofluids are shown in Eq. (5)[26]:

$$\left(\rho C_p\right)_{hnf} = (1 - \phi_2)\left[(1 - \phi_1)\left(\rho C_p\right)_f + \phi_1\left(\rho C_p\right)_{s_1}\right]$$
$$\mu_{hnf} = \frac{\mu_f}{(1 - \phi_1)^{2.5}(1 - \phi_2)^{2.5}}$$
$$\frac{k_{hnf}}{k_{nf}} = \frac{k_{s_2} + 2k_{nf} - 2\phi_2\left(k_{nf} - k_{s_2}\right)}{k_{s_2} + 2k_{nf} + \phi_2\left(k_{nf} - k_{s_2}\right)}, \frac{k_{nf}}{k_f} = \frac{k_{s_1} + 2k_f - 2\phi_{s_1}(k_f - k_{s_1})}{k_{s_1} + 2k_f + \phi_{s_1}(k_f - k_{s_1})}, \tag{5}$$
$$\frac{\sigma_{hnf}}{\sigma_{bf}} = \left[\frac{\left(\sigma_{s_2} - \sigma_{bf}\right)3\phi_{s_2}}{\left(\sigma_{s_2} + 2\sigma_{bf}\right) + \left(\sigma_{bf} - \sigma_{s_2}\right)\phi_{s_2}} + 1\right], \frac{\sigma_{bf}}{\sigma_f} = \left[\frac{\left(\sigma_f - \sigma_{s_1}\right)3\phi_{s_1}}{\left(\sigma_{s_1} - \sigma_f\right) - \left(\sigma_{s_1} + 2\sigma_f\right)} + 1\right],$$
$$\rho_{hnf} = (1 - \phi_2)\left[(1 - \phi_1)(\rho)_f + \phi_1(\rho)_{s_1}\right] + \phi_2(\rho)_{s_2}.$$

Considering Takhar et al.[44], the group of similar variables is defined as:

$$u = axf'(\eta) + bx^2g'(\eta), v = -\sqrt{av_f}f(\eta) - \frac{2bx}{\sqrt{\frac{a}{v_f}}}g(\eta), \theta(\eta) = \frac{T - T_\infty}{T_w - T_\infty}, \eta = y\sqrt{\frac{a}{v_f}}, \tag{6}$$

Hence that:

$$v_w = -\sqrt{av_f}S_1 - \frac{2bx}{\sqrt{\frac{a}{v_f}}}S_2 \tag{7}$$

Here, S_1, S_2 are the transpiration parameters with $(S_1, S_2) > 0$ for suction and $(S_1, S_2) < 0$ for blowing and injection constraint. By using the Eq. (5), Eqs. (2, 3) are changed to:

$$f''' - (1-\phi_1)^{2.5}(1-\phi_2)^{2.5}(1-\phi_2)\left[\left[(1-\phi_1)(\rho)_f + \phi_1(\rho)_{s_1}\right] + \phi_2(\rho)_{s_2}\right]$$
$$\beta\left(2f'''f' - ff^{iv} - f'^2\right) - ff'' + f'^2 - (1-\phi_1)^{2.5}(1-\phi_2)^{2.5}\frac{\sigma_{hnf}}{\sigma_f}Mf' = 0, \tag{8}$$

$$g''' - fg'' + 3f'g' - 2gf'' - (1-\phi_1)^{2.5}(1-\phi_2)^{2.5}(1-\phi_2)\left[\left[(1-\phi_1)(\rho)_f + \phi_1(\rho)_{s_1}\right] + \phi_2(\rho)_{s_2}\right]$$
$$\beta\left(3f'g''' + 3f'''g' - 2gf^{iv} - 3f''g'' - fg^{iv}\right) - (1-\phi_1)^{2.5}(1-\phi_2)^{2.5}\frac{\sigma_{hnf}}{\sigma_f}Mg' = 0, \tag{9}$$

$$(g')^2 - gg'' + (1-\phi_1)^{2.5}(1-\phi_2)^{2.5}(1-\phi_2)\left[\left[(1-\phi_1)(\rho)_f + \phi_1(\rho)_{s_1}\right] + \phi_2(\rho)_{s_2}\right]\beta\left((g'')^2 + gg^{(iv)} - 2g'g'''\right) = 0, \tag{10}$$

$$\frac{\frac{k_{hnf}}{k_f}}{\frac{(\rho cp)_{hnf}}{(\rho cp)_f}}\left(\theta'' + R\left[(1 + (\theta_w - 1)\theta)^3\theta''\right]\right) + \Pr\left(f + k_1 g\right)\theta' = 0, \tag{11}$$

Subjected to the conditions:

$$f(0) = S_1, g(0) = S_2, f'(0) = \lambda, g'(0) = \lambda, \theta(0) = 1,$$
$$f'(\infty) \to 0, g'(\infty) \to 0, \theta(\infty) \to 0. \tag{12}$$

$$M = \frac{\sigma_f B_0^2}{a\rho_f}, \Pr = \frac{\upsilon_f}{\alpha_f}, R = \frac{16\sigma^* T_\infty^3}{3k_{nf}k^*}, \theta_w = \frac{T_w}{T_\alpha}, \beta_1 = \frac{\alpha_1}{\rho_f ax^2}. \tag{13}$$

Above the symbols $M, \beta, \Pr, R, \theta_w$ and $k_1 = \frac{cx}{a}$ respectively denote magnetic parameter, second grade fluid parameter, Prandtl number, radiation parameter, temperature ratio parameter and nonlinear stretching parameter.

Quantities of engineering interest. The engineering quantities of interest are C_{fx} and Nu_x that is denoted as[16];

$$C_{fx} = \frac{\tau_w}{\rho(ax)^2}, Nu_x = \frac{xq_w}{k_f(T_w - T_\infty)}, \tag{14}$$

The surface heat flux q_w and τ_w are written as;

$$\tau_w = \frac{\mu_{hnf}}{\rho_f}(u_y)_{y=0}, q_w = -k_{hnf}(T_y)_{y=0} + (qr)_w, \tag{15}$$

By the use of Eqs. (13) and (14), then we have;

$$C_{fx}Re_x^{\frac{1}{2}} = \frac{\mu_{hnf}}{\mu_{nf}}\left[f''(0) + \beta_1 xg''(0)\right], Nu_x Re_x^{-\frac{1}{2}} = -\frac{k_{hnf}}{k_f}(1 + R\theta_w^3)\theta'(0). \tag{16}$$

Above $Re_x = \frac{\upsilon_f}{ax^2}$ depicts local Reynolds number while β_1 is a dimension free parameter with $\beta_1 = \frac{b}{a}$.

Solution by HAM
The problem is explained through the HAM[60–63] method. The detail of HAM for current modeled problem is describes as follows:

$$L_{\widehat{f}}(\widehat{f}) = \widehat{f}''', L_{\widehat{\theta}}(\widehat{\theta}) = \widehat{\theta}'', \tag{17}$$

Linear operators $L_{\widehat{f}},$ and $L_{\widehat{\theta}}$ are signified as

$$L_{\widehat{f}}(e_1 + e_2\eta + e_3\eta^2) = 0, L_{\widehat{\theta}}(e_4 + e_5\eta) = 0, \tag{18}$$

The constant non-linear operators are $N_{\widehat{f}}$ and $N_{\widehat{\theta}}$ with

$$N_{\widehat{f}}\left[\widehat{f}(\eta; \zeta)\right] = \widehat{f}_{\eta\eta\eta} - (1-\phi_1)^{2.5}(1-\phi_2)^{2.5}(1-\phi_2)\left[\left[(1-\phi_1)(\rho)_f + \phi_1(\rho)_{s_1}\right] + \phi_2(\rho)_{s_2}\right]$$
$$\beta\left(2\widehat{f}_\eta\widehat{f}_{\eta\eta\eta\eta} + \widehat{f}_{\eta\eta}^2 - \widehat{f}\widehat{f}_{\eta\eta\eta\eta}\right) - \widehat{f}\widehat{f}_{\eta\eta} + \left(\widehat{f}_\eta\right)^2 - (1-\phi_1)^{2.5}(1-\phi_2)^{2.5}\frac{\sigma_{hnf}}{\sigma_f}M\widehat{f}_\eta \tag{19}$$

$$
\mathrm{N}_{\widehat{g}}\left[\widehat{g}(\eta;\zeta)\right] = \widehat{g}_{\eta\eta\eta} - (1-\phi_1)^{2.5}(1-\phi_2)^{2.5}(1-\phi_2)\left[\left[(1-\phi_1)(\rho)_f + \phi_1(\rho)_{s_1}\right] + \phi_2(\rho)_{s_2}\right]
$$

$$
\beta\left(3\widehat{f}_\eta\widehat{g}_{\eta\eta\eta} + 3\widehat{f}_{\eta\eta\eta}\widehat{g}_\eta - \widehat{f}\widehat{g}_{\eta\eta\eta\eta} - 3\widehat{f}_{\eta\eta}\widehat{g}_{\eta\eta} - 2\widehat{f}_{\eta\eta\eta\eta}\widehat{g}\right) - \widehat{f}\widehat{g}_{\eta\eta} + 3\widehat{f}_\eta\widehat{g}_\eta - 2\widehat{f}_{\eta\eta}\widehat{g}
$$

$$
- (1-\phi_1)^{2.5}(1-\phi_2)^{2.5}\frac{\sigma_{hnf}}{\sigma_f}M\widehat{g}_\eta,
\tag{20}
$$

$$
\mathrm{N}_{\widehat{\theta}}\left[\widehat{f}(\eta;\zeta),\widehat{\theta}(\eta;\zeta),\right] = \frac{\frac{k_{hnf}}{k_f}}{\frac{(\rho cp)_{hnf}}{(\rho cp)_f}}\left[\frac{1}{\Pr}\widehat{\theta}_{\eta\eta} + R\left(1 + (\theta_w - 1)\widehat{\theta}\right)^3\widehat{\theta}_{\eta\eta} + 3\left(1 + (\theta_w - 1)\widehat{\theta}\right)^2(\theta_w - 1)\widehat{\theta}_\eta^2\right] + (f+g)\widehat{\theta}_\eta,
\tag{21}
$$

For Eqs. (8–10) the 0th-order system is written as

$$
(1-\eta)\mathrm{L}_{\widehat{f}}\left[\widehat{f}(\eta;\zeta) - \widehat{f}_0(\eta)\right] = p\hbar_{\widehat{f}}\mathrm{N}_{\widehat{f}}\left[\widehat{f}(\eta;\zeta)\right]
\tag{22}
$$

$$
(1-\eta)\mathrm{L}_{\widehat{g}}\left[\widehat{g}(\eta;\zeta) - \widehat{g}_0(\eta)\right] = p\hbar_{\widehat{g}}\mathrm{N}_{\widehat{g}}\left[\widehat{g}(\eta;\zeta)\right]
\tag{23}
$$

$$
(1-\eta)\,\mathrm{L}_{\widehat{\theta}}\left[\widehat{\theta}(\eta;\zeta) - \widehat{\theta}_0(\eta)\right] = p\hbar_{\widehat{\theta}}\mathrm{N}_{\widehat{\theta}}\left[\widehat{f}(\eta;\zeta),\widehat{\theta}(\eta;\zeta)\right]
\tag{24}
$$

whereas BCs are:

$$
\widehat{f}(\eta;\zeta)\Big|_{\eta=0} = S_1,\ \widehat{g}(\eta;\zeta)\Big|_{\eta=0} = S_2\ \frac{\partial\widehat{f}(\eta;\zeta)}{\partial\eta}\Big|_{\eta=0} = \lambda,\ \frac{\partial\widehat{g}(\eta;\zeta)}{\partial\eta}\Big|_{\eta=0} = \lambda,\ \widehat{\theta}(\eta;\zeta)\Big|_{\eta=0} = 1,
$$

$$
\frac{\partial\widehat{f}(\eta;\zeta)}{\partial\eta}\Big|_{\eta=\infty} = 0,\ \frac{\partial\widehat{g}(\eta;\zeta)}{\partial\eta}\Big|_{\eta=\infty} = 0,\ \widehat{\theta}(\eta;\zeta)\Big|_{\eta=\infty} = 0,\ \widehat{\phi}(\eta;\zeta)\Big|_{\eta=\infty} = 0.
\tag{25}
$$

While the implanting constraint is $\zeta \in [0,1][0,1]$, to adjust for the solution convergence $\hbar_{\widehat{f}}$, $\hbar_{\widehat{g}}$ and $\hbar_{\widehat{\theta}}$ are utilized. When $\zeta = 0$ and $\zeta = 1$ we have:

$$
\widehat{f}(\eta;1) = \widehat{f}(\eta),\widehat{g}(\xi;1) = \widehat{g}(\eta),\widehat{\theta}(\eta;1) = \widehat{\theta}(\eta)
\tag{26}
$$

Enlarge the $\widehat{f}(\eta;\zeta),\widehat{g}(\eta;\zeta)$ and $\widehat{\theta}(\eta;\zeta)$ over Taylor's series for $\zeta = 0$

$$
\widehat{f}(\eta;\zeta) = \widehat{f}_0(\eta) + \sum_{n=1}^\infty \widehat{f}_n(\eta)\zeta^n
$$

$$
\widehat{g}(\eta;\zeta) = \widehat{g}_0(\eta) + \sum_{n=1}^\infty \widehat{g}_n(\eta)\zeta^n
\tag{27}
$$

$$
\widehat{\theta}(\eta;\zeta) = \widehat{\theta}_0(\eta) + \sum_{n=1}^\infty \widehat{\theta}_n(\eta)\zeta^n\eta
$$

$$
\widehat{f}_n(\eta) = \frac{1}{n!}\frac{\partial\widehat{f}(\eta;\zeta)}{\partial\eta}\Big|_{p=0},\ \widehat{g}_n(\eta) = \frac{1}{n!}\frac{\partial\widehat{g}(\eta;\zeta)}{\partial\eta}\Big|_{p=0}\ \widehat{\theta}_n(\eta) = \frac{1}{n!}\frac{\partial\widehat{\theta}(\eta;\zeta)}{\partial\eta}\Big|_{p=0}.
\tag{28}
$$

whereas BCs are:

$$
\widehat{f}(0) = S_1,\widehat{g}(0) = S_2,\widehat{f'}(0) = \lambda,\widehat{g'}(0) = \lambda,\widehat{\theta}(0) = 1,\widehat{f'}(\infty) = 0,\widehat{g'}(\infty) = 0,\widehat{\theta}(\infty) = 0.
\tag{29}
$$

where

$$
\text{While } \chi_n = \begin{cases} 0, & \text{if } n \leq 1 \\ 1, & \text{if } n > 1. \end{cases}
\tag{30}
$$

Results and discussions

In this section, we now deliberate the different outcomes of the existing study and displayed graphically in Figs. 2, 3, 4, 5, 6, 7, 8, 9, 10 and 11. Figure 1 shows the Schematic representation of the flow problem. The influence of magnetic factor M on these velocity distributions is reflected in Figs. 2 and 3. It is witnessed in Fig. 2 that axial velocity distributions is declining with amassed estimations of magnetic factors. The intensification in M indicates
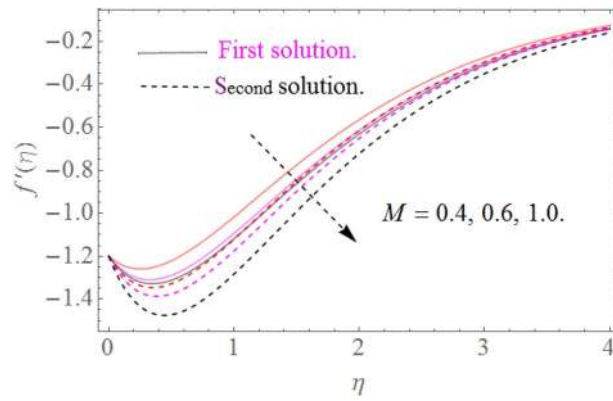
Figure 2. Influence of M on $f'(\eta)$ for $Re_x = 5, \beta = 0.2, \phi_2 = 0.02$.
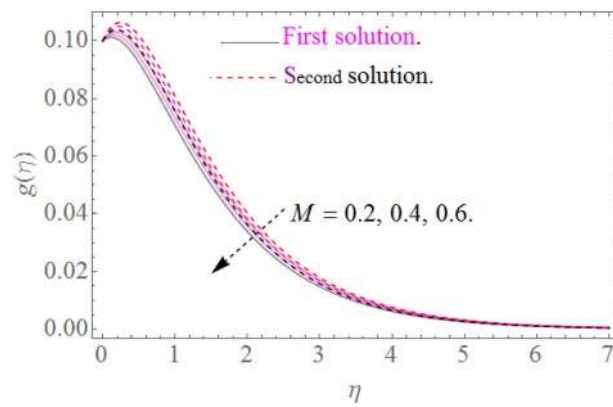

Figure 3. Influence of M on $g(\eta)$ for $Re_x = 5, \beta = 0.2, \phi_2 = 0.02$.
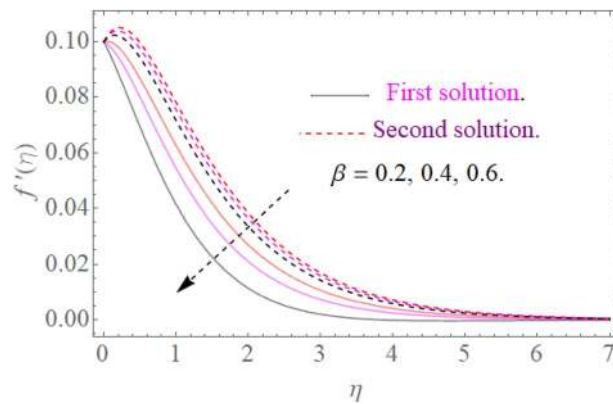

Figure 4. Influence of β on $f'(\eta)$ for $M = 0.9, \phi_2 = 0.02$.

to expanding Lorentz force which is because of the interface of electric and magnetic fields in motion of electrically directed liquid. We can also say that bigger Lorentz force deals more resistance to the transportation phenomenon, that is why upsurge in M agrees to a decline in velocity distributions. On the other hand a tangential component $g(\eta)$ is also declines with an expansion in estimations of M as presented in Fig. 3. Figures 4 and 5 depict the influence of β on $f'(\eta)$ and $g(\eta)$. We see from Figs. 4 and 5 that the $f'(\eta)$ and $g(\eta)$ decline against β. It is evident that for higher assessment of β the viscosity of fluid improves and accordingly velocity $f'(\eta)$ and $g(\eta)$ increase. In fact, the second grade parameter β improves the non-Newtonian behavior for its larger vales and consequently declines the velocity profile. The flow profiles in Fig. 6 suggest that augmentation in momentum
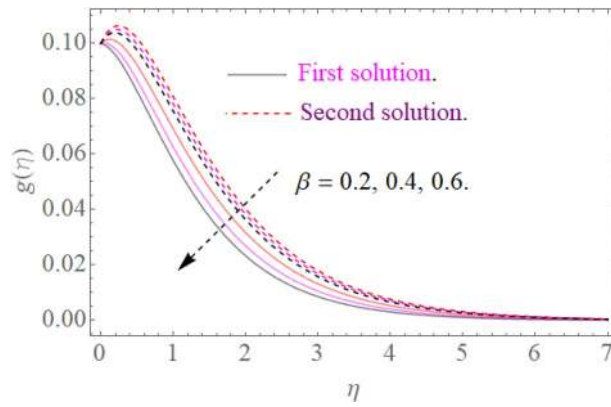
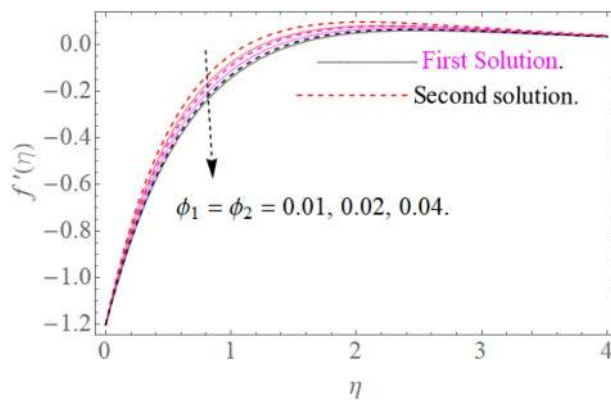**Figure 5.** Influence of β on $g(\eta)$ for $M = 0.9, \phi_2 = 0.02$.

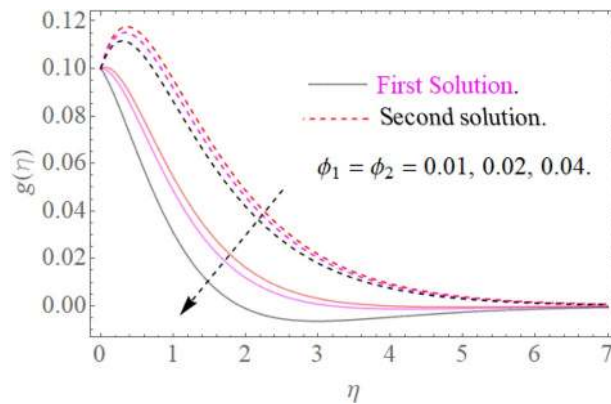**Figure 6.** Influence of ϕ_2 on $f'(\eta)$ for $M = 0.9, \beta = 0.2$.

Figure 7. Influence of ϕ_2 on $g(\eta)$ for $M = 0.9, \beta = 0.2$.

limit layer viscosity declines the flow and gradient in flow of fluid. Moreover, the thicker the momentum limit layer proposes the little wall shear stress as a result of which $f'(\eta)$ reduces with a corresponding increase in ϕ_1, ϕ_2. Figure 7 shows the impact of ϕ_2 on $g(\eta)$. The larger magnitude of the volume fraction ϕ_1 and ϕ_2 improve the resistive force and consequently declines the velocity field $g(\eta)$.

Temperature profile. Figure 8 indicates that $\theta(\eta)$ reduces with Pr impact. It is additionally certain that expansion in the Pr prompts diminishing the limit of thermal layer thickness. Actually Prandtl number is inversely proportional to diffusivity of thermal boundary layer; hence increase in the values of Pr results in
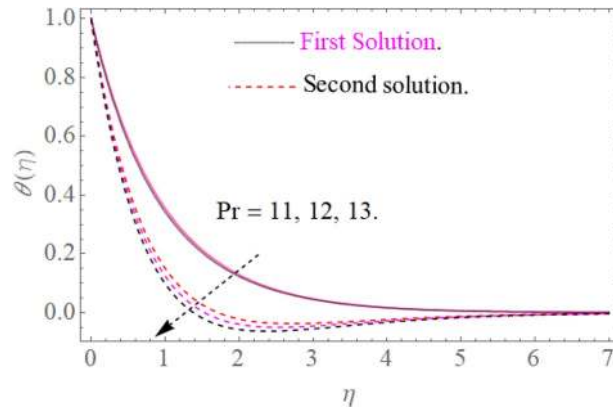
Figure 8. Influence of Pr on $\theta(\eta)$ for $R = 0.3, \theta_w = 1.2$.
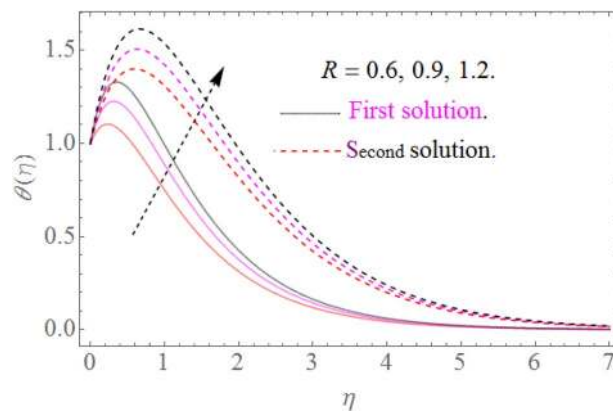

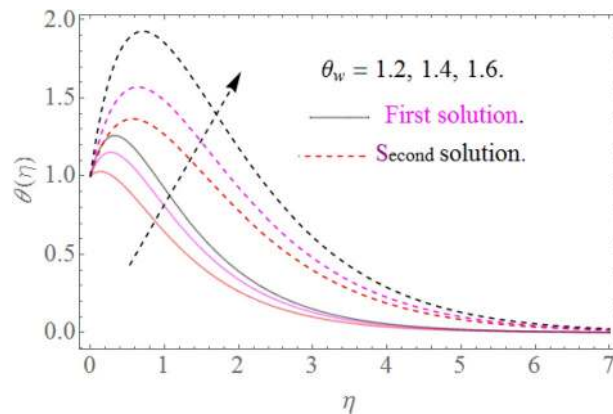**Figure 9.** Influence of R on $\theta(\eta)$ for $\text{Pr} = 10.2, \theta_w = 1.2$.

Figure 10. Impact of θ_w on $\theta(\eta)$ for $R = 0.3, \text{Pr} = 10.2$.

decline of thermal characteristics. So that $\theta(\eta)$ for extending sheet reduces by growing Pr. Figure 9 detects that the distribution $\theta(\eta)$ increases as R upsurges with the datum that the rate of energy transmission jumps up due to increase in thermal radiations. Figure 10 observes that the temperature profiles $\theta(\eta)$ increase as θ_w increases because θ_w is the ratio of the hybrid nanofluid temperature at the sheet surface to the ambient temperature of the liquid. Figure 11 observes that the temperature profiles $\theta(\eta)$ increase as ϕ_1, ϕ_2 increase. The larger magnitude of the parameters ϕ_1, ϕ_2 enhancing the thermal efficiency of the base fluid and consequently the temperature profile increases.
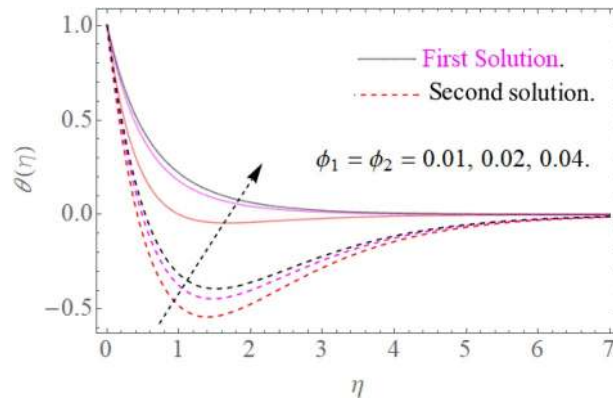
Figure 11. Influence of ϕ_1, ϕ_2 on $\theta(\eta)$ for $R = 0.3$, $\mathrm{Pr} = 10.2$.

S1	S2	β	M	ϕ_1	ϕ_2	$C_{fx}Re_x^{\frac{1}{2}}$
0.25	0.30	0.40	0.45	0.01	0.01	0.4177710
0.30						0.4195709
0.35						0.4213785
	0.30					0.4177710
	0.35					0.4113878
	0.40					0.4049111
		0.40				0.4497204
		0.45				0.4497374
		0.50				0.4497888
			0.40			0.4565509
			0.45			0.4597204
			0.50			0.4628635
				0.03		0.4155745
				0.04		0.4166816
				0.05		0.4177710
					0.03	0.4193832
					0.04	0.42316718
					0.05	0.42839318

Table 2. Outcome of different physical factors over Skin friction $C_{fx}Re_x^{\frac{1}{2}} = \frac{\mu_{hnf}}{\mu_{nf}}\left[f''(0) + \beta x g''(0)\right]$.

Table discussion.   Table 2 shows the influence of various physical constraints on skin friction of the hybrid nanofluid flow. From Table 2 it is realized that the increase of the nanoparticle percentage in the base fluid boosts the skin friction of the base fluid. The parameters S_1 and S_2 are respiration parameters or injection and suction parameters of the nanofluid if we inject more fluid, then skin friction enhances. When we apply the orthogonal magnetic field to the flow of the hybrid nanofluid; this magnetic field attracts the metallic nanoparticles due to which the skin fraction increases. Skin friction enhances with the larger magnitude of the second grade parameter β.

Table 3 displays the influence of various physical factors on the Nusselt number. Nusselt number means the flow rate of the heat. From Table 3 we clearly see that if we enhance the Prandtl number then by physical definition of the Prandtl number when it enhances, the thermal conductivity of the fluid decreases, therefore the heat transfer rate declines with the enhancement of the Prandtl number. The addition in the thermal radiation factor improves the heat transfer rate. From Table 3 we clearly see that with the enhancement of the parameters ϕ_1, ϕ_2, θ_w improve the heat transfer rate. It has been observed that the hybrid nanofluids are the most efficient to improve the heat transfer rate as compared to the traditional fluids. Tables 4 and 5 are displayed to validate the obtained results with the existing literature. The Nusselt number and skin friction of the present study are compared and closed agreement is obtained.

Pr	R	θ_w	ϕ_1	ϕ_2	$Nu_x Re_x^{-\frac{1}{2}}$
10	0.3	0.2	0.05	0.03	0.4877173
11					0.4827149
12					0.4773147
	0.3				0.4946563
	0.6				0.4957187
	0.9				0.4971463
		0.2			
		0.4			
		0.6			
			0.05		
			0.06		
			0.07		
				0.03	
				0.04	
				0.05	

Table 3. Influence of dissimilar physical constraints over Nusselt number $Nu_x Re_x^{-\frac{1}{2}}$.

	$C_{fx} Re_x^{\frac{1}{2}}$ [Results of Ref.[15]]	$C_{fx} Re_x^{\frac{1}{2}}$ [Results of Ref.[16]]	$C_{fx} Re_x^{\frac{1}{2}}$ [Present results]
0.4	0.4186600	0.4189483	
0.5	0.4437524	0.4438372	0.4428635
0.6	0.4726413	0.4727261	0.4717524
0.7	0.5015302	0.5015150	0.50028413

Table 4. Comparison of the present work with the published work[15,16].

	$Nu_x Re_x^{-\frac{1}{2}}$ [Results of Ref.[17]]	$Nu_x Re_x^{-\frac{1}{2}}$ [Present results]
10	0.4889312	0.4877173
11	0.4867101	0.4827149
12	0.4745012	0.4773147

Table 5. Comparison of the present work with the published work[17].

Conclusions

The magnetohydrodynamic second-grade hybrid nanofluid flow towards an extending/shrinking sheet with thermal radiation is inspected in this investigation. The main concern of this research work is to consider the hybrid nanofluid which is perceived by hanging two distinctive nanoparticles known as alumina and copper within the second grade fluid while the fluid motion is formed from the non-linearly stretching/shrinking sheet.

The important observations are given below.

- Second-grade fluid used as a base fluid for the solid nanoparticles and the influence of the second grade parameter β observed versus the velocity field.
- Al_2O_3 and Cu are used as the solid nanoparticles. The increments in the volume fraction ϕ_1 and ϕ_2 of the nanoparticles increase the thermal efficiency of the fluid.
- For greater values of M the velocity $f'(\eta)$ and $g(\eta)$ decrease.
- The heat transfer rate upsurges for bigger Rd and θ_w.
- The heat transfer rate diminishes with augmentation of Prandtl number.
- The velocity profile declines for the larger magnitude of the Reynolds number.
- It has been observed that the hybrid nanofluids are most efficient to enhance the thermal conductivity of the second grade fluids as compared to the traditional fluids.

Data availability

The data that support the findings of this study are available from the corresponding author upon reasonable request.

References

1. Choi, S. U. S. Enhancing thermal conductivity of fluids with nanoparticles. *Proc. ASME Int. Mech. Eng. Congr. Expo.* **66**, 99–105 (1995).
2. Akbar, N. S., Nadeem, S., Hayat, T. & Hendi, A. A. Peristaltic flow of a nanofluid with slip effects. *Meccanica* **47**, 1283–1294 (2012).
3. El-Sayed, M. F., Harouna, M. H. & Mostapha, D. R. Electro convection peristaltic flow of viscous dielectric liquid sheet in asymmetrical flexible channel. *J. Atomization Sprays* **25**, 985–1011 (2015).
4. Nakhchi, M. E. & Esfahani, J. A. Cu–water nanofluid flow and heat transfer in a heat exchanger tube equipped with cross-cut twisted tape. *Powder Technol.* **339**, 985–994 (2018).
5. Sheremet, M. A. & Pop, I. Marangoni natural convection in a cubical cavity filled with a nanofluid: Buongiorno'snanofluid model. *J. Therm. Anal. Calorim.* **135**, 357–369 (2019).
6. Mahian, O. *et al.* Recent advances in modelling and simulation of nanofluid flows-Part I: fundamentals and theory. *Phys. Rep.* **790**, 1–48 (2019).
7. Dinarvand, S., Hosseini, R. & Pop, I. Axisymmetric mixed convective stagnation-point flow of a nanofluid over a vertical permeable cylinder by Tiwari-Das nanofluid model. *Powder Technol.* **311**, 147–156 (2017).
8. Ramasubramaniam, R., Chen, J. & Liu, H. Homogeneous carbon nanotube/polymer composites for electrical applications. *Appl. Phys.* **83**, 2928–2930 (2003).
9. Xue, Q. Z. Model for thermal conductivity of carbon nanotube-based composites. *Phys. B* **368**, 302–307 (2005).
10. Nadeem, S. Single wall carbon nanotube (SWCNT) analysis on peristaltic flow in an inclined tube with permeable walls. *Int. J. Heat Mass Transfer.* **97**, 794–802 (2016).
11. Hayat, T., Ahmed, S., Muhammad, T., Alsaedi, A. & Ayub, M. Computational modeling for homogeneous-heterogeneous reactionsin three-dimensional flow of carbon nanotubes. *Results Phys.* **7**, 2651–2657 (2017).
12. Nadeem, S., Khan, A. U. & Hussain, S. T. Model based study of SWCNT and MWCNT thermal conductivities effect on the heat transfer due to the oscillating wall conditions. *Int. J. Hydrog. Energy* **42**, 45–57 (2017).
13. Sheikholeslami, M. New computational approach for exergy and entropy analysis of nanofluid under the impact of Lorentz force through a porous media. *Comput. Methods Appl. Mech. Eng.* **344**, 319–333 (2019).
14. Sheikholeslami, M. Numerical approach for MHD Al2O3-water nanofluid transportation inside a permeable medium using innovative computer method. *Comput. Methods Appl. Mech. Eng.* **344**, 306–318 (2019).
15. Cortell, R. A novel analytic solution of MHD flow for two classes of visco-elastic fluid over a sheet stretched with non-linearly (quadratic) velocity. *Meccanica* **48**, 2299–2310 (2013).
16. Cortell, R. MHD (magneto-hydrodynamic) flow and radiative nonlinear heat transfer of a viscoelastic fluid over a stretching sheet with heat generation/absorption. *Energy* **74**(1), 896–905 (2014).
17. Mahapatra, T. R. & Sidui, S. An analytical solution of MHD flow of two visco-elastic fluids over a sheet shrinking with quadratic velocity. *Alex. Eng. J.* **55**(1), 163–168 (2016).
18. Gul, T., Bilal, M., Shuaib, M., Mukhtar, S. & Thounthong, P. Thin film flow of the water-based carbon nanotubes hybrid nanofluid under the magnetic effects. *Heat Trans.* **49**, 3211–3227 (2020).
19. Sheikholeslami, M., Ganji, D. D. & Ashorynejad, H. R. Investigation of squeezing unsteady nanofluid flow using ADM. *Powder Technol.* **239**, 259–265 (2013).
20. Jawad, M. *et al.* Impact of nonlinear thermal radiation and the viscous dissipation effect on the unsteady three-dimensional rotating flow of single-wall carbon nanotubes with aqueous suspensions. *Symmetry* **11**, 1–18 (2019).
21. Turcu, R. *et al.* New polypyrrole-multiwalled carbon nanotubes hybrid materials. *Mat. J. Optoelectron. Adv. Mater.* **8**, 643–647 (2006).
22. Suresh, S., Venkitaraj, K. P., Selvakumar, P. & Chandrasekar, M. Synthesis of Al2O3-Cu/water hybrid nanofluids using two step method and its thermo physical properties. *Colloids Surf A* **388**, 41–48 (2011).
23. Suresh, S., Venkitaraj, K. P., Selvakumar, P. & Chandrasekar, M. Effect of Al2O3-Cu/water hybrid nanofluid in heat transfer. *Exp. Therm Fluid Sci.* **38**, 54–60 (2012).
24. I. Waini, A. Ishak, I. Pop, MHD flow and heat transfer of a hybrid nanofluid past a permeable stretching/shrinking wedge, Appl. Math. Mech. (English Ed.). 1–14 (2020).
25. Waini, I., Ishak, A. & Pop, I. Hybrid nanofluid flow towards a stagnation point on an exponentially stretching/shrinking vertical sheet with buoyancy effects. *Int. J. Numer. Methods Heat Fluid Flow* https://doi.org/10.1108/HFF-02-2020-0086 (2020).
26. Zainal, N. A., Nazar, R., Naganthran, K. & Pop, I. Unsteady three-dimensional MHD nonaxisymmetricHomann stagnation point flow of a hybrid nanofluid with stability analysis. *Mathematics* **8**, 1–25 (2020).
27. Safwa Khashi'ie, N., MdArifin, N., Pop, I. & Syahirah Wahid, N. Flow and heat transfer of hybrid nanofluid over a permeable shrinking cylinder with Joule heating: a comparative analysis. *Alex. Eng. J.* https://doi.org/10.1016/j.aej.2020.04.048 (2020).
28. Khashiie, N. S. *et al.* Three dimensional hybrid nanofluid flow and heat transfer past a permeable stretching/shrinking sheet with velocity slip and convective condition. *Chin. J. Phys.* https://doi.org/10.1016/j.cjph.2020.03.032 (2020).
29. Das, P. K. A review based on the effect and mechanism of thermal conductivity of normal nanofluids and hybrid nanofluids. *J. Mol. Liq.* **240**, 420–446 (2017).
30. Miroshnichenko, I. V., Sheremet, M. A., Oztop, H. F. & Abu-Hamdeh, N. Natural convection of Al2O3/H2O nanofluid in an open inclined cavity with a heat-generating element. *Int. J. Heat Mass Transf.* **126**, 184–191 (2018).
31. Siavashi, M. & Rostami, A. Two-phase simulation of non-Newtonian nanofluid natural convection in a circular annulus partially or completely filled with porous media. *Int. J, Mech. Sci.* **133**, 689–703 (2017).
32. Huminic, G. & Huminic, A. Hybrid nanofluids for heat transfer applications—a state-of the-art review. *Int. J. Heat Mass Transf.* **125**, 82–103 (2018).
33. Dinarvand, S. Nodal/saddle stagnation-point boundary layer flow of CuO–Ag/water hybrid nanofluid: a novel hybridity model. *Microsyst. Technol.* **25**, 2609–2623 (2019).
34. Dinarvand, S. & Rostami, M. N. An innovative mass-based model of aqueous zinc oxide–gold hybrid nanofluid for von karman's swirling flow: a comprehensive report on effects of nanoparticle shape factor. *J. Therm. Anal. Calorim.* **138**, 845–855 (2019).
35. Tayebi, T. & Chamkha, A. J. Free convection enhancement in an annulus between horizontal confocal elliptical cylinders using hybrid nanofluids. *Numer. Heat Transfer Part A* **70**, 1141–1156 (2016).
36. Suresh, S., Venkitaraj, K. P., Selvakumar, P. & Chandrasekar, M. Effect of Al2O3–Cu/water hybrid nanofluid in heat transfer. *Exp. Therm. Fluid Sci.* **38**, 54–60 (2012).

37. Jena, P. K., Brocchi, E. A. & Motta, M. S. In-situ formation of Cu–Al$_2$O$_3$ nano-scale composites by chemical routes and studies on their microstructures. *Mater. Sci. Eng. A* **313**, 180–186 (2001).

38. Afshari, A., Akbari, M., Toghraie, D. & Yazdi, M. E. Experimental investigation of rheological behavior of the hybrid nanofluid of MWCNT–alumina/water (80%)–ethylene-glycol (20%). *J. Therm. Anal. Calorim.* **132**, 1001–1015 (2018).

39. Ramzan, M. *et al.* Unsteady MHD carbon nanotubes suspended nanofluid flow with thermal stratification and nonlinear thermal radiation. *Alex. Eng. J.* **59**, 1557–1566 (2020).

40. Barnoon, P., Toghraie, D. & Karimipour, A. Application of rotating circular obstacles in improving ferrofuid heat transfer in an enclosure saturated with porous medium subjected to a magnetic fled. *J. Therm. Anal. Calorim.* https://doi.org/10.1007/s10973-020-09896-1 (2020).

41. Afrand, M. Davood Toghraie, Arash Karimipour, Somchai Wongwises, A numerical study of natural convection in a vertical annulus filled with gallium in the presence of magnetic field. *J. Magn. Magn. Mater.* **430**, 22–28 (2017).

42. Barnoon, P., Toghraie, D., Dehkordi, R. B. & Abed, H. MHD mixed convection and entropy generation in a lid-driven cavity with rotating cylinders filled by a nanofluid using two phase mixture model. *J. Magn. Magn. Mater.* **483**, 224–248 (2019).

43. Farzinpour, M., Toghraie, D., Mehmandoust, B., Aghadavoudi, F. & Karimipour, A. Molecular dynamics study of barrier effects on Ferro-nanofluid flow in the presence of constant and time-dependent external magnetic fields. *J. Mol. Liq.* **308**, 1–7 (2020).

44. Mousavi, S. E., Moshfegh, A., Afrouzi, H. H., Javadzadegan, A. & Toghraie, D. Simulation of droplet detachment from hydrophobic and hydrophilic solid surfaces under the electric field using Lattice Boltzmann Method (LBM). *J. Mol. Liq.* **313**, 1–14 (2020).

45. Turkyilmazoglu, M. Single phase nanofluids in fluid mechanics and their hydrodynamic linear stability analysis. *Comput. Methods Programs Biomed.* https://doi.org/10.1016/j.cmpb.2019.105171 (2019).

46. Turkyilmazoglu, M. Convergence accelerating in the homotopy analysis method: a new approach. *Adv. Appl. Math. Mech.* **10**, 925–947 (2018).

47. Turkyilmazoglu, M. An effective approach for approximate analytical solutions of the damped Duffing equation. *Phys. Scr.* **86**, 1–6 (2012).

48. Turkyilmazoglu, M. Latitudinally deforming rotating sphere. *Appl. Math. Model.* **71**, 1–11 (2019).

49. Shah, N. A. *et al.* Significance of suction and dual stretching on the dynamics of various hybrid nanofluids: comparative analysis between type I and type II models. *Phys. Scr.* **95**, 095205 (2020).

50. Sheikholeslami, M., Farshad, S. A. & Shafee, A. Houman Babazadeh Performance of solar collector with turbulator involving nanomaterial turbulent regime. *Renew. Energy* **163**, 1222–1237 (2020).

51. Sheikholeslami, M. & Farshad, S. A. Nanoparticle transportation inside a tube with quad-channel tapes involving solar radiation. *Powder Technol.* **378**, 145–159 (2020).

52. Mondal, S. *et al.* A theoretical nanofuid analysis exhibiting hydromagnetics characteristics employing CVFEM. *J. Braz. Soc. Mech. Sci. Eng.* https://doi.org/10.1007/s40430-019-2103-2 (2020).

53. Hashemi-Tilehnoee, M., Dogonchi, A. S., Seyyedi, S. M. & Sharifpur, M. Magneto-fluid dynamic and second law analysis in a hot porous cavity filled by nanofluid and nano-encapsulated phase change material suspension with different layout of cooling channels. *J. Energy Storage* **31**, 1–14 (2020).

54. Tlilia, I., Seyyedi, S. M., Dogonchi, A. S., Hashemi-Tilehnoee, M. & Ganji, D. D. Analysis of a single-phase natural circulation loop with hybrid-nanofluid. *Int. Commun. Heat Mass Transfer* **112**, 1–13 (2020).

55. Cortell, R. A novel analytic solution of MHD flow for two classes of viscoelastic fluid over a sheet stretched with non-linearly (quadratic) velocity. *Meccanica* **48**, 2299–2310 (2013).

56. Nasir, N. A. A. M., Ishak, A., Pop, I. & Zainuddin, N. MHD stagnation point flow towards a quadratically stretching/shrinking surface. *J. Phys. Conf. Ser.* **1366**, 1–9 (2019).

57. Koriko, O. K., Adegbie, K. S., Animasaun, I. L. & Ijirimoye, A. F. Comparative analysis between three-dimensional flow of water conveying alumina nanoparticles and water conveying Alumina–Iron(III) oxide nanoparticles in the presence of Lorentz force. *Arab. J. Sci. Eng.* https://doi.org/10.1007/s13369-019-04223-9 (2019).

58. Vaidya, H. *et al.* Influence of transport properties on the peristaltic MHD Jeffrey fluid flow through a porous asymmetric tapered channel. *Results Phys.* **18**, 1–13 (2020).

59. Aly, E. H. & Pop, I. MHD flow and heat transfer over a permeable stretching/shrinking sheet in a hybridnanofluid with a convective boundary condition. *Int. J. Numer. Methods Heat Fluid Flow* **29**, 3012–3038 (2019).

60. Liao, S. J. An optimal homotopy-analysis approach for strongly nonlinear differential equations. *Commun. Nonlinear Sci. Numer. Simul.* **15**, 2003–2016 (2010).

61. Liao, S. J. *Advances in the Homotopy Analysis Method* (World Science Press, Singapore, 2013).

62. Khan, W., Idress, M., Gul, T., Khan, M. A. & Bonyah, E. Three non-Newtonian fluids flow considering thin film over an unsteady stretching surface with variable fluid properties. *Adv. Mech. Eng.* **10**(10), 1–7 (2018).

63. Gul, T. *et al.* Magnetic dipole impact on the hybrid nanofluid flow over an extending surface. *Sci. Rep.* **10**, 8474. https://doi.org/10.1038/s41598-020-65298-1 (2020).

Acknowledgements

Author contributions

M.J., A.S. and A.K. modeled and solved the problem. M.J. and A.S. wrote the manuscript. Z.S., T.G. and A.T. contributed in the numerical computations and plotting the graphical results. Z.S., P.K., A.S. and T.G. work in the revision of the manuscript. All the corresponding authors finalized the manuscript after its internal evaluation.

Competing interests

The authors declare no competing interests.

Additional information

Correspondence and requests for materials should be addressed to P.K. or Z.S.

Reprints and permissions information is available at www.nature.com/reprints.

Publisher's note Springer Nature remains neutral with regard to jurisdictional claims in published maps and institutional affiliations.